JOURNAL OF SOLID STATE CHEMISTRY **133,** 536–544 (1997)
ARTICLE NO. SC977530

On the Crystallography and Thermodynamics in Orientationally Disordered Phases in Two-Component Systems

J. Salud,* D. O. López,* M. Barrio,* J. Ll. Tamarit,*,[1] H. A. J. Oonk,† P. Negrier,‡ and Y. Haget‡

*Departament de Física i Enginyeria Nuclear, Universitat Politècnica de Catalunya, ETSEIB,[2] Diagonal, 647, 08028 Barcelona, Catalonia, Spain;
†Petrology Group, Faculty of Earth Sciences,[2] Budapestlaan, 4, NL-3584 CD Utrecht, The Netherlands;
‡Laboratoire de Physique Moléculaire Optique et Hertzienne, URA 283 CNRS, Université Bordeaux I,[2] 351, Cours de la Libération, 33405 Talence, France

Received February 10, 1997; in revised form June 30, 1997; accepted June 30, 1997

The experimental two-component phase diagram between the orientationally disordered crystals 2-amino-2-methyl-1,3-propanediol (AMP) and 1,1,1-tris(hydroxymethyl)propane (PG) has been established from room temperature to the liquid state using thermal analysis and X-ray powder diffraction techniques. The intermolecular interactions in the orientationally disordered mixed crystals of the mentioned system and other related two-component systems are discussed by analyzing the evolution of the packing coefficient as a function of the the composition. A thermodynamic analysis of the presented phase diagram and the redetermined AMP/NPG (2,2-dimethyl-1,3-propanediol) is reported on the basis of the enthalpy–entropy compensation theory. © 1997 Academic Press

1. INTRODUCTION

Orientationally disordered crystals (ODICs) are molecular crystals characterized by high rotational mobility of molecules and low entropy of fusion (1). To understand the nature of the phases displaying such disorder, also called plastic phases, it is important to delve further into the molecular interactions that govern both structural and thermodynamic properties. To do so, several techniques have been applied to date to pure substances, such as NMR, neutron diffraction, and dielectric relaxation (2–4). Moreover, additional studies by means of techniques that are able to modify the intermolecular distances, such as high-pressure measurements, have been undertaken (5).

Another powerful way to modify the molecular surroundings is to introduce a foreign substance (6–8). In experimental practice this comes down to the study of binary systems. On this line of reasoning the present paper is devoted to the study of two binary systems of which the pure-component substances have ODICs. The systems are AMP/PG and AMP/NPG, where AMP = $NH_2(CH_3)C(CH_2OH)_2$, PG = $(CH_3)C(CH_2OH)_3$, and NPG = $(CH_3)_2C(CH_2OH)_2$. Because the ODIC form of AMP (body-centered cubic) is different from the ODIC form of the others (face-centered cubic), there are two types of molecular alloy. In terms of the phase diagrams this corresponds to the presence of two simple-(ODIC) phase fields separated by a two-phase region.

In this study the phase behaviour of the two systems is examined from the viewpoints of crystallography and thermodynamics. As for the aspect of crystallography special attention is given to the packing coefficient. With regard to the thermodynamic analysis a main part is devoted to the phenomenon of enthalpy–entropy compensation (9). Both packing coefficient and enthalpy–entropy compensation have become, in recent years, key issues in the study of mixed crystalline materials (10–14). The present paper underlines their importance and at the same time provides new experimental evidence.

2. EXPERIMENTAL

2.1. Materials

The substances were purchased from Aldrich Chemical Company with purities of 99.5% for AMP [2-amino-2-methyl-1,3-propanediol, $NH_2(CH_3)C(CH_2OH)_2$] and 99% for NPG [2,2-dimethyl, 1-3-propanediol, $(CH_3)_2C(CH_2OH)_2$] and PG[1,1,1-tris(hydroxymethyl)propane, $(CH_3)C(CH_2OH)_3$]. They were subjected to additional purification through repeated vacuum sublimation at 343, 353, and 393 K, respectively; the result was controlled by differential scanning calorimetry.

Two-component mixtures were prepared from the melt of the materials in the selected proportions by slow cooling to room temperature. The samples invariably were treated under a controlled Ar atmosphere.

[1]To whom correspondence should be addressed.
[2]All members of REALM.

0022-4596/97 $25.00

2.2. Diffraction at Constant Temperature

X-ray powder diffraction measurements were performed using a Siemens D-500 vertical diffractometer equipped with an Anton–Paar TTK temperature camera ($\pm$ 0.5 K). The experimental conditions and the procedure have been described elsewhere (6, 15).

2.3. Diffraction as a Function of the Temperature

Powder diffraction measurements as a function of the continuous evolution of the temperature were made by means of a Guinier–Simon camera with Cu$K\alpha$ radiation, quartz monochromator, window width of 1 mm, film speed of 1 mm h^{-1}, and heating rates between 1 and 9 K h^{-1}. The powdered samples were sealed in Lindemann glass capillaries of 0.50-mm diameter.

2.4. Thermal Analysis

Thermal analysis was carried out by means of a Perkin–Elmer DSC-7 instrument, using a scanning rate of 2 K min^{-1} and ca. 5-mg sample masses hermetically sealed into aluminum crucibles under a controlled Ar atmosphere.

3. RESULTS

3.1. Polymorphism of the Pure Components

3.1.1. AMP $[NH_2(CH_3)C(CH_2OH)_2]$

The crystal structure of the low-temperature ordered form, phase II (hereafter denoted as M_1), is monoclinic with $Z = 4$ (16). Lattice parameters at 293 K are $a = 8.613(3)$ Å, $b = 11.037(4)$ Å, $c = 6.105(2)$ Å, and $b = 93.57(1)^\circ$ (17). X-ray powder diffraction measurements at 313 K yielded the refined lattice parameters $a = 8.621(4)$ Å, $b = 11.053(5)$ Å, $c = 6.141(5)$ Å, and $\beta = 93.64(1)^\circ$.

At 353.0 $\pm$ 1.0 K monoclinic AMP transforms into an orientationally disordered phase, the symmetry of which is body-centered cubic with $Z = 2$ (C_I). The latter phase is stable up to the melting at 384.7 $\pm$ 1.0 K. The cubic lattice parameter at 363 K has been determined to be 6.777(8) Å (17). The entropy changes for phase M_1-to-C_I and C_I-to-liquid transitions are 64.3 $\pm$ 1.8 and 7.0 $\pm$ 0.3 J K^{-1} mol^{-1}, respectively (18).

3.1.2. PG $[(CH_3)C(CH_2OH)_3]$

X-ray diffraction studies carried out on the ordered low temperature form (Q) between 293 and 393 K provided the lattice parameters for a tetragonal unit cell with space group $I\bar{4}$ and $Z = 2$ (19). The high temperature orientationally disordered form, which is stable between 356.6 $\pm$ 1.0 K and the melting point (473.7 $\pm$ 1.0 K), has face-centered cubic symmetry with $Z = 4$ (denoted as C_F) with a lattice parameter of 8.876(8) Å at 363 K (20, 21).

The entropy changes associated with the solid–solid transition and melting are 58.6 $\pm$ 5.0 and 10.0 $\pm$ 0.2 J K^{-1} mol^{-1}, respectively (18).

3.1.3. NPG $[(CH_3)_2C(CH_2OH)_2]$

The low-temperature form ($P2_1/c$, referred to as M_2) of NPG transforms at 314.3 $\pm$ 1.0 K to an orientationally disordered form, the symmetry of which is face-centered cubic (C_F) (22). The latter phase is stable to the melting point at 402.8 $\pm$ 1.0 K. Lattice parameters as well as thermodynamic data have been published elsewhere (23).

3.2. Two-Component Systems

3.2.1. AMP/PG Phase Diagram

3.2.1.1. Diffraction as a function of temperature. The Guinier–Simon patterns corresponding to the samples with PG mole fractions (X) of 0.40 and 0.55 together with those of the pure components AMP and PG are presented in Fig. 1.

For the sample with $X = 0.40$ the successive domains may be described as (i) the existence of a two-phase domain $[M_1 + Q]$; (ii) at ca. 321 K, disappearance of the reflections corresponding to the tetragonal Q phase and appearance of the cubic C_I phase giving rise to a $[M_1 + C_I]$ domain; (iii) at 330 K, disappearance of the M_1 phase. The $X = 0.55$ mixtures display the following features with increasing temperature: (i) transition from $[M_1 + Q]$ to $[Q + C_I]$ at ca. 321 K, (ii) disappearance of C_I and appearance of C_F at 326–328 K giving rise to a $[Q + C_F]$ two-phase domain; (iii) at higher temperatures, transformation of the $[Q + C_F]$ domain to a $[C_F]$ one-phase domain, i.e., to an orientationally disordered molecular alloy.

From the evidence displayed by the Guinier–Simon patterns it follows that there are two eutectoid invariants, $[M_1 + Q + C_I]$ and $[Q + C_I + C_F]$, at about 322 and 328 K, respectively. Owing to the small distance between the two invariants on the temperature scale, the instrument was set at the lowest possible scanning rate (1 K h^{-1}) and film speed (1 mm h^{-1}).

We were not able to make a proper registration of the transition from plastic crystalline solid to liquid. This has to do with large (differences in) vapor pressures which give rise to large concentration changes in the capillaries (at 390 K the equilibrium vapor pressures of pure AMP and PG are 72.77 and 11.10 Pa, respectively) (24).

3.2.1.2. Diffraction at constant temperature. This study was undertaken with two goals: first, to confirm the existence of the two detected close eutectoid invariants, and

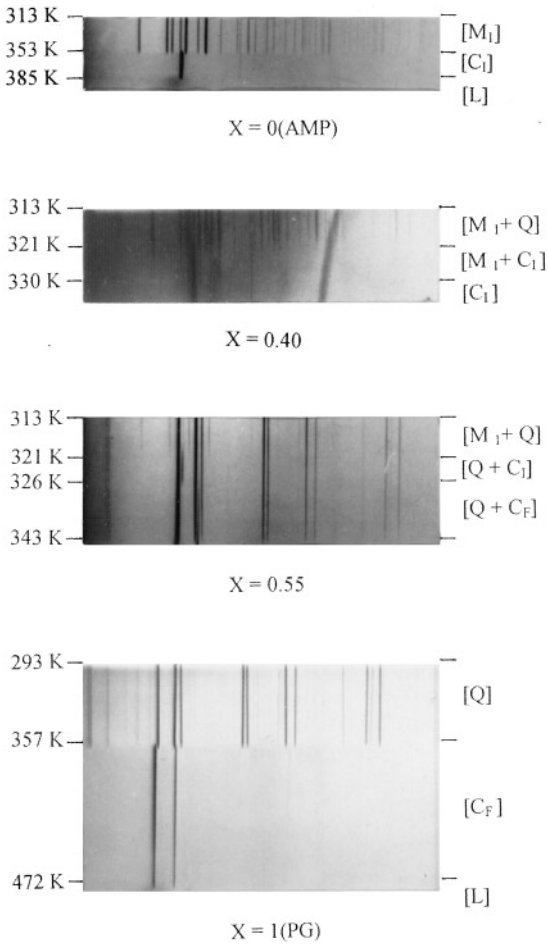

FIG. 1. Guinier–Simon patterns corresponding to the pure compounds AMP and PG and the samples $X = 0.40$ and $X = 0.55$.

second, to delimit the range of the $[M_1 + Q]$ and $[C_I + C_F]$ two-phase domains.

To verify the existence of the two invariants, several mixtures were studied at several temperatures. Figure 2

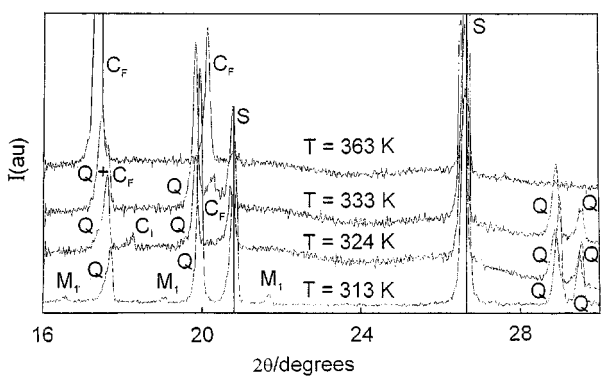

FIG. 2. 2θ window of the diffraction patterns for $X = 0.80$ at 313, 324, 333, and 363 K.

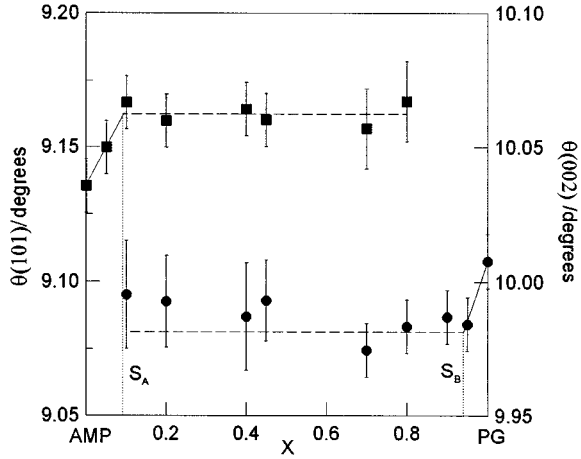

FIG. 3. Bragg angles, θ (degrees), as a function of the mole fraction (X) for the (101) (■) and (002) (●) reflections of the monoclinic and tetragonal lattices, respectively, at 313 K in the AMP/PG system.

shows a 2θ window of the diffraction patterns at 313, 324, 333, and 363 K. The successive domains $[M_1 + Q]$, $[Q + C_I]$, $[Q + C_F]$, and $[C_F]$ are clearly observed for a sample with a mole fraction of $X = 0.80$.

a. The solubility boundaries of the AMP and PG components at 313 K were established by studying the positions of the more intense reflections corresponding to the monoclinic M_1 and tetragonal Q lattices. Figure 3 depicts, as an example, the positions of the (101) and (002) reflections of the M and Q lattices, respectively, as a function of mole fraction. From the evolution of the angle positions of the reflections versus concentration, the solubility boundaries have been found to be $S_A(313\text{ K}) \cong 0.09$, i.e., the molecular alloy $AMP_{0.91}PG_{0.09}$, and $S_B(313\text{ K}) \cong 0.96$, i.e., $AMP_{0.04}PG_{0.96}$. Despite the small differences in the Bragg angles between the pure compounds and the average values of the samples belonging to the two-phase domain the lattice parameters of such limiting solid solutions were refined: $a = 8.633(4)$ Å, $b = 11.080(5)$ Å, $c = 6.112(5)$ Å, and $\beta = 93.61(1)^\circ$ for the monoclinic solid solution, and $a = 6.055(2)$ Å and $c = 8.880(3)$ Å for the tetragonal one.

b. Figure 4 depicts the evolution of the Bragg angles of the (110) and (111) reflections corresponding to the bcc and fcc lattices at 363 K. Following the same procedure as in the previous case, the evolutions enabled us to establish the limits of the two-phase region between the two orientationally disordered single phase fields: $S_A(363\text{ K}) \cong 0.44$ and $S_B(363\text{ K}) \cong 0.54$.

The two-phase region between the two low-temperature forms and the one between the two high-temperature orientationally disordered phases are necessarily present owing to the nonisomorphous nature of the related phases. In addition it may be accented that the widths of the two types of two-phase regions are quite different: about 0.85 on the

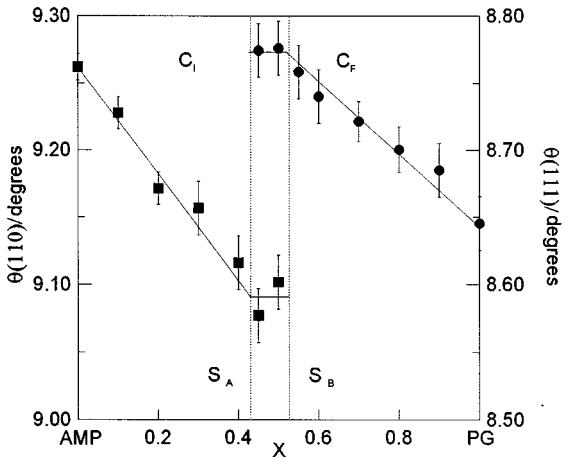

FIG. 4. Bragg angles, θ (degrees), as a function of the mole fraction (X) for the (110) (left side, ■) and (111) (right side, ●) reflections corresponding to the bcc and fcc lattices, respectively, at 363 K in the AMP/PG system.

mole fraction scale for the low-temperature form and about 0.10 for the high-temperature form. This experimental result is known to be the normal behavior of two-component systems of which the pure-component subtances have ODICs (10, 23).

3.2.1.3. Thermal Analysis. Accurate transition and melting temperatures were determined by means of thermal analysis, confirming the general trends observed by the diffraction studies.

The complete set of experimental data was used to construct the phase diagram represented by Fig. 5. The eutectoid invariants were set at 323.2 ± 1.0 K and 330.2 ± 1.5 K.

3.2.2. AMP/NPG Phase Diagram

Although the experimental AMP/NPG two-component system has been previously published by several authors (17, 25), a subsequent thermodynamic analysis has revealed some thermodynamic incoherences. These arise basically from the impossibility of accounting for the one- and two-phase low-temperature domains by means of the Gibbs energy functions calculated from the high-temperature equilibria. Disturbed by these incoherences we decided to redetermine the phase diagram, taking great care of the purity of the materials. The redetermined phase diagram, represented by Fig. 6, has the same global features as the one published earlier, but it has no more incoherences as shown below (Section 4.2). The temperatures of the (reestablished) eutectoid invariants are 293.7 ± 1.0 and 325.0 ± 1.2 K.

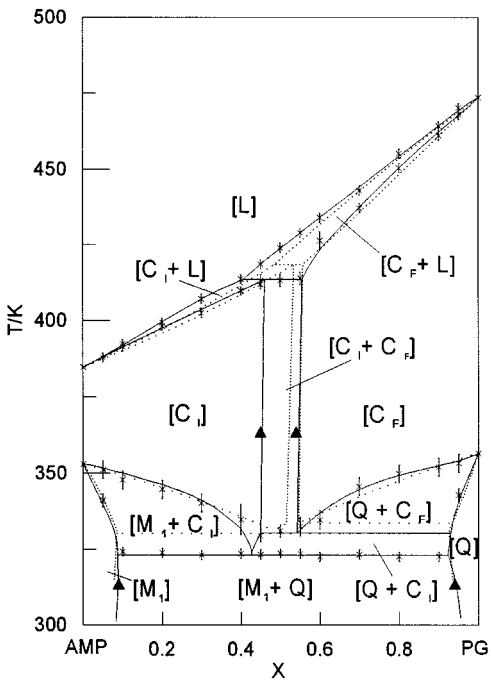

FIG. 5. Experimental and calculated (dotted line) phase diagrams of the the binary system AMP/PG: (×) DSC, (Δ) solubility boundaries determined by X-ray powder diffraction at constant temperature.

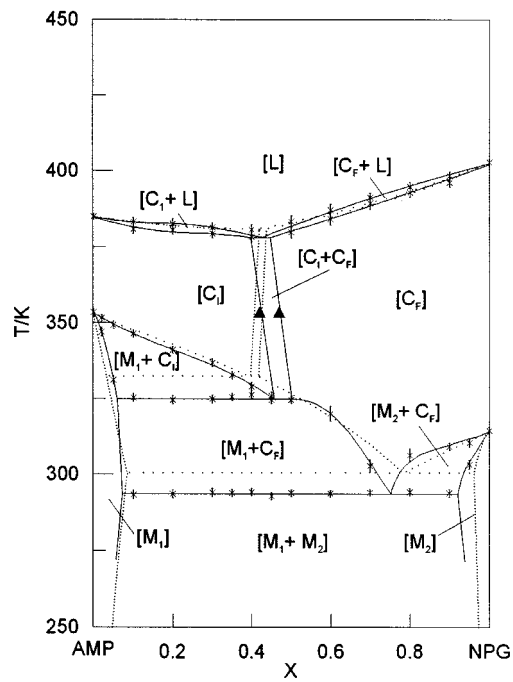

FIG. 6. Experimental and calculated (dotted line) phase diagrams of the binary system AMP/NPG: (×) DSC, (Δ) solubility boundaries determined by X-ray powder diffraction at constant temperature.

4. DISCUSSION

4.1. Intermolecular Interactions in the Disordered Molecular Alloys

In a recent paper, we showed that the intermolecular interactions by hydrogen bonds play an important role in the orientationally disordered phases (10). In particular, we extensively studied the molecular alloys formed between nonisomorphous plastic phases corresponding to some chemically and structurally related compounds formed by tetrahedral molecules belonging to two series $(CH_3)_{4-n}(CH_2OH)_n$, for $n = 1, \ldots, 4$ and $(NH_2)(CH_3)_{3-n}C(CH_2OH)_n$, for $n = 2$ and 3 (6, 17, 26). The compounds of the first series crystallize on cooling from the melt in a fcc lattice, whereas for those of the second series, the lattice corresponds to bcc symmetry. When mixing two compounds of the two different series, i.e., isomorphism is not displayed in the ODIC state, the intermolecular interactions by means of the hydrogen bonds control the packing of the mixed crystals in such a way that the packing coefficient of the molecular alloys (both bcc and fcc) increases with increasing number of CH_2OH and NH_2 groups in the average molecule of the alloy. Moreover, it was clearly shown by studying the PE/TRIS $[C(CH_2OH)_4/(NH_2)C(CH_2OH)_3]$ two-component system in the high-temperature disordered forms that the packing coefficient remains constant as a function of the molar fraction (6). This is to say that the strengths of the hydrogen bonds produced by the NH_2 group and those of the CH_2OH group become more or less equal in the disordered phases. To confirm the last assumption, the study of the packing coefficient evolution in the AMP/PG system is interesting, seeing that the total numbers of groups able to form hydrogen bonds in the considered molecules are equal: two CH_2OH groups and one NH_2 group in the AMP molecule and three CH_2OH groups in the PG molecule.

Considering the definition of packing coefficient, $\kappa(X) = V_m(X)/V_z(X)$, where V_m is the volume of an isolated molecule and V_z the volume of the crystal lattice per molecule, its calculation should be done by the experimental determination of V_z and by taking a model for the V_m value. The $V_z(X)$ values for the AMP/PG system can be straightforwardly calculated from the lattice parameter evolution, determined previously by means of X-ray powder diffraction at 363 K. The simplest way to calculate $V_m(X)$ is to set the average of the volumes of the isolated molecules participating in the alloy, i.e., the volume of the statistical entity,

$$V_m(X) = (1 - X)V_{mA} + XV_{mB}.$$

The volumes of the molecules considered have been calculated elsewhere [for details, see Refs. (10, 23)]. Figure 7 gives the evolution of the packing coefficient as a function of mole fraction for the two kinds of molecular alloy (bcc and fcc) and corresponding to the previously reported PE/Tris system (6) and for the AMP/PG system presented in this work. It is obvious that the packing parameter evolutions are almost flat for each kind of molecular alloy, showing that the substitution of the molecules does not produce any (perceptible) modification in the intermolecular interaction scheme. Moreover, we want to emphasize the relatively high values of the packing parameter for the pure compounds as well as for their alloys, which rules out incompatibility between high packing and the existence of orientational disorder (27).

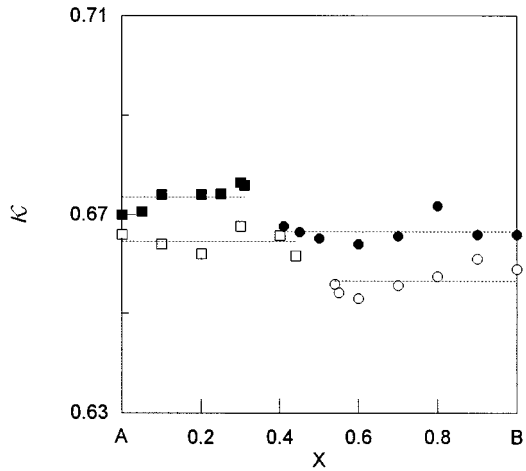

FIG. 7. Packing coefficient (κ) for the bcc (□, ■) and fcc (○, ●) molecular alloys corresponding to the two-component systems TRIS/PE (full symbols: ■, at 428 K; ● at 453 K) and AMP/PG (empty symbols: at 363 K).

4.2. Application of the Enthalpy–Entropy Compensation Theory

Under isobaric conditions, the thermodynamic properties of a binary system are known if for each of its forms the Gibbs energy of the pure substances is known as a function of temperature and the excess Gibbs energy of the mixture as a function of temperature and composition. The excess Gibbs energy, as any Gibbs energy, is composed of an enthalpy part and an entropy part,

$$G^E(T, X) = H^E(T, X) - T \cdot S^E(T, X), \qquad [1]$$

where X stands for mole fraction of the second component.

In the thermodynamic analysis that follows special attention is given to the phenomenon of enthalpy (H)–entropy (S) compensation (9, 12). The simplest way to formulate a compensation law is to define the excess Gibbs energy as a product of a temperature-dependent and system-independent factor $g(T)$ and a temperature-independent and

system-dependent factor $f(A_i)$, A_i being a collection of parameters describing a particular system of the class. In such a way, the excess Gibbs energy may be written

$$G^{E}(T, X) = g(T) \cdot f(A_i, X). \quad [2]$$

As the excess Gibbs energy must go through zero at the same temperature (T_c, the compensation temperature) for all the systems in the class, a suitable form for the $g(T)$ function is

$$g(T) = 1 - T/T_c. \quad [3]$$

With regard to $f(A_i, X)$ and taking into account the possible asymmetry on the concentration dependence of the excess Gibbs energy, the simplest $f(A_i, X)$ function may be defined as

$$f(A_i, X) = A_1 X(1 - X)\,[1 + A_2(1 - 2X)], \quad [4]$$

where A_1 and A_2 are the parameters that describe a particular system of a class. Moreover, it should be noted that the chosen form accounts directly for the magnitude (A_1) and for the asymmetry (A_2) of the excess Gibbs energy.

Inserting Eqs. [3] and [4] into Eq. (2) leads to the following expression for the excess Gibbs energy:

$$G^{E}(T, X) = (1 - T/T_c)\, A_1 X(1 - X)\,[1 + A_2(1 - 2X)]. \quad [5]$$

According to the selected formalism, the compensation temperature is the proportionality constant between excess enthalpy (H^E) and excess entropy (S^E), which follow from Eq. [5] as

$$H^{E}(T, X) = H^{E}(X) = A_1 X(1 - X)[1 + A_2(1 - 2X)] \quad [6a]$$

$$S^{E}(T, X) = S^{E}(X) = A_1 X(1 - X)[1 + A_2(1 - 2X)]/T_c. \quad [6b]$$

In the case of the two-component systems analyzed here, the components have different lattice symmetry in the orientationally disordered phases, either bcc or fcc, implying that they are nonisomorphous. Thus, each kind of solid solution will be described by means of an excess Gibbs energy of the form of [5] with different A_i parameters. The nonisomorphism of the disordered phases present gives rise to the existence of two different orientationally disordered liquid equilibrium loops in both of the considered phase diagrams. The metastable extensions of these loops end in the theoretical metastable melting points of the pure substances corresponding to a phase that is assumed to be isomorphous with the phase for which the extension of the loop is done. To estimate the fcc and bcc metastable melting points of the AMP and PG metastable phases, the narrow stable $[C_F + L]$ and $[C_I + L]$ branches in the AMP/PG system were extrapolated to $X = 1$ and $X = 0$, respectively, by means of a simple procedure in terms of the equal-Gibbs-curve (EGC) method (28, 29). The values of the metastable points determined are summarized in Table 1. The same procedure used to determine the metastable melting points provides the differences in the excess Gibbs energy functions between the disordered and liquid phases. Because not only differences in the excess Gibbs energies but also specific values of these functions are required to calculate the ordered–disordered phase equilibria, some assumptions have to be made about the excess properties of the liquid solution. In want of such values we have neglected the excess Gibbs energies of the liquid mixtures; thus the minus ΔG^E functions were identified with the G^E functions for the mixed orientationally disordered states.

To determine the temperature dependence of the G^E function, i.e., the value of the compensation temperature, the derived excess Gibbs energy data have to be combined with the excess enthalpy data. At a given temperature T, the relation

$$T_c = T/(1 - G^{E}(T, X)/H^{E}(X)) \quad [7]$$

can be directly derived from expressions [6a] and [5]. Exact excess enthalpy data are rather difficult to obtain. Nevertheless, the heat of melting as a function of the mol fraction for the AMP/PG system has been measured (see Fig. 8) in each solid solution domain. Assuming the temperature-independent excess enthalpy form of Eq. [6a] and according to the

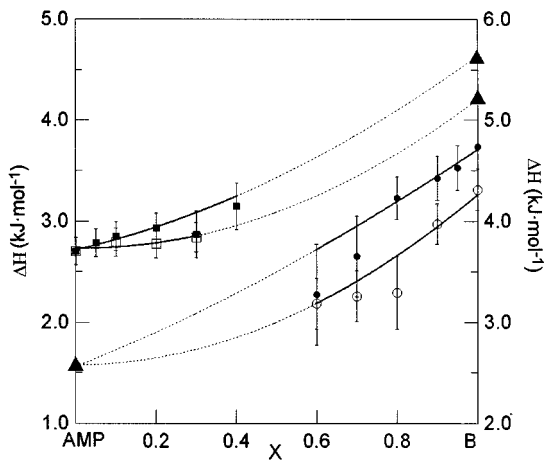

FIG. 8. Enthalpies of melting for the bcc (□, ■, right side) and fcc (○, ●, left side) molecular alloys corresponding to the two-component systems AMP/PG (B ≡ PG, full symbols) and AMP/NPG (B ≡ NPG, empty symbols). The triangles correspond to the calculated metastable values.

nonexistence of excess values for the liquid solution, the excess enthalpy for each solid solution was obtained by fitting a second-order polynomial to the experimental data displayed in Fig. 8. Combining the results for H^E and G^E, the value of $T_c \cong 800$ K is obtained for both bcc and fcc alloys in the AMP/PG system. The procedure used needs to fix the enthalpy of melting corresponding to metastable phases. These values were obtained by taking the entropy of melting to be the same as that of the stable form. The values obtained are included in Table 1.

Finally, the excess Gibbs energy and T_c values are used to determine the A_1 and A_2 parameters for the two orientationally disordered phases. These values are summarized in Table 1. It is important to note that, from a thermodynamic point of view, the temperature dependence is similar for both bcc and fcc molecular alloys in this AMP/PG system, as shown from the same value of temperature T_c. Similar findings, equal T_c temperature values for a large number of two-component systems of alkanes have been recently reported (30).

For the AMP/NPG phase diagram a more or less similar procedure was followed. In this case, taking notice of the close behavior of bcc and fcc molecular alloys in the previous analyzed system, we assume that the alloys of the AMP/NPG system have the same compensation temperature, i.e., $T_c = 800$ K. The system-dependent A_1 and A_2 parameters for each kind of solid solution in this system are collected in Table 1.

The miscibility in the ordered low-temperature forms of both AMP/PG and AMP/NPG systems is almost negligible (see Figs. 5 and 6, respectively), so then, the complete phase diagrams were calculated by using the excess Gibbs energies corresponding to the disordered high-temperature forms previously determined. The final resulting phase diagrams calculated by means of the ProPhase program (31) are shown in Figs. 5 and 6. Attempts to improve the agreement between calculated and experimental phase diagrams were performed by considering the limited miscibility in the ordered forms, but no noticeable improvements were reached.

Notwithstanding the difficulty of calculating the presented phase diagrams (due to the relatively poor experimental data and accessibility to some parameters needed to perform the thermodynamic analysis), our goal has been to find a compromise between physical significance and agreement between calculated and experimental phase diagrams for the orientationally disordered phases. From this point of view, the agreement can be considered as satisfactory (see Table 2) and the coherence of the model, i.e., the representation of the physical reality, can be considered valid. In Fig. 8 we show the experimental and the calculated enthalpies of melting for the bcc and fcc molecular alloys of the AMP/NPG system. It should be mentioned that in the calculation of this phase diagram the T_c value was assumed to be exactly the same as in the previous one (AMP/PG) by assuming that the two binary systems belong to the same class. So then, the experimental values of the excess enthalpy for the AMP/NPG system were considered, and notwithstanding, the agreement between calculated and experimental excess enthalpy values is satisfactory (see Fig. 8).

From a thermodynamic analysis point of view, the calculation problems can be divided into two types: (i) the determination of the metastable properties (as melting temperature and melting enthalpy) corresponding to the isomorphous metastable phases of the compounds which have to be considered to build up the needed crossed isodimorphism; (ii) the model itself used. With regard to this

TABLE 1
Temperatures and Enthalpies of Melting of the Stable (s) and Metastable (m) bcc and fcc Forms Together with the Calculated Values of the System-Dependent A_1 and A_2 Parameters of the Binary Systems AMP/PG and AMP/NPG

		AMP/PG	AMP/NPG
bcc	T_1 (K)	384.7 (s)	384.7 (s)
	T_2 (K)	465.0 (m)	393.1 (m)
	ΔH_1 (J mol^{-1})	2700 (s)	2700 (s)
	ΔH_2 (J mol^{-1})	4650 (m)	4206 (m)
	A_1 (J mol^{-1})	1003	584
	A_2	− 0.23	− 0.33
fcc	T_1 (K)	363.5 (m)	363.5 (m)
	T_2 (K)	473.7 (s)	402.8 (s)
	ΔH_1 (J mol^{-1})	2552 (m)	2552 (m)
	ΔH_2 (J mol^{-1})	4737 (s)	4310 (s)
	A_1 (J mol^{-1})	860	296
	A_2	0.06	− 1.33

TABLE 2
Comparison between Experimental (E) and Calculated (C) Invariant Equilibria

System	Invariant		T (K)	X_M	X_N	X_P
AMP/NPG	Eutectoid	E	293.7	0.05	0.75	0.92
		C	300.5	0.09	0.79	0.98
	Eutectoid	E	325.0	0.06	0.46	0.51
		C	332.5	0.04	0.40	0.42
	Eutectic	E	377.5	0.38	0.42	0.44
		C	380.8	0.41	0.42	0.43
AMP/PG	Eutectoid	E	323.0	0.09	0.43	0.92
		C	330.0	0.09	0.47	0.92
	Eutectoid	E	330.2	0.44	0.53	0.93
		C	333.5	0.51	0.54	0.96
	Peritectic	E	413.6	0.40	0.47	0.57
		C	418.4	0.48	0.53	0.56

fact, it can be seen that, for both phase diagrams, the most discordant results concern the two-phase regions between the two orientational single phase fields which produce a considerable difference between calculated and experimentally determined eutectic (case of the AMP/NPG) and peritectic (case of the AMP/PG) invariants, 3.3 and 5.3 K, respectively. Such discrepancies are basically produced by the selected form of the temperature-dependent system-independent factor $g(T)$. This choice, in addition to the temperature-independent excess enthalpy and entropy expressions, does not allow fitting of the two-phase regions, these being a direct consequence of the excess Gibbs energies determined from the orientationally disordered liquid phase equilibria.

An empirical estimation method for the enthalpy–entropy compensation temperature in terms of a quasi-subregular solution model including a compensation law was published (32). From the experimental evidence of a large variety of mixtures relating molecular mixtures (such as *p*-dihalobenzenes, alkali halides, alkaline earth oxides, and cryogenic noble gases), the equation

$$T_c = (4.0 \pm 0.16)\, T_1 T_2/(T_1 + T_2), \qquad [8]$$

in which T_1 and T_2 are the melting temperatures of the first and second components in the mixture, was derived. It should be mentioned that for all the mixtures used isomorphism was supposed to exist; i.e., one Gibbs energy curve was sufficient to describe the behavior of the solid solutions. This is not the case for the systems presented in this paper, so then, the empirical relation [8] must be used carefully. In particular, the enthalpy–entropy compensation temperature is associated with each solid solution domain, and then, expression [8] should be applied by using the stable and metastable temperatures of the solid solutions considered. If such a method is followed the T_c calculated by Eq. [8] are 842 and 778 K for the bcc alloys and 823 and 764 K for the fcc alloys for the AMP/PG and AMP/NPG systems, respectively. By averaging the calculated values, a temperature of 802 K is obtained, which is certainly close to the value calculated from the thermodynamic analysis performed (800 K). However, this excellent agreement may be circumstantial because Eq. [8] was obtained from thermodynamic analysis of solid–liquid equilibria where a large number of the molecular alloys did not display orientational disorder.

In a more general framework T_c values were calculated for a set of independent systems (14). From this study it follows that the enthalpy–entropy compensation temperature is above the melting range for each of the considered systems. Such experimental evidence was mathematically expressed by means of the quotient $\log T_c/\log T_{EGC}$ $(X = 0.5) = 1.10 \pm 0.05$, where $T_{EGC}(X = 0.5)$ represents the temperature of the equal-Gibbs curve at $X = 0.5$ (29). For some binary systems such as *l*-carvoxime + *d*-carvoxime, and gold + palladium, the quotient differs significantly from the rule (1.03 and 1.04, respectively). More recently, two sets of orientationally disordered mixed crystals were the subject of a similar thermodynamic analysis; for the first set, relating two-component systems displaying complete miscibility (33) (i.e., isomorphism being proved), the calculated quotient is about 1.09; however, for the second set (13), where the enclosed systems display crossed isodimorphism as in the systems of the present work, the quotient (about 0.97) differs from the mean by somewhat more than the standard deviation. At present, a still unpublished work (34) relating ODIC mixed crystals between CBr_4 and C_2Cl_6 compounds shows close behavior, more precisely, a quotient of 1.01. For the two-component systems determined in the present work the quotients, the accuracy of which is somewhat limited, can be considered as satisfactory due to the carefully performed thermodynamic analysis and are 1.12 and 1.11 for AMP/NPG and AMP/PG systems, respectively. It may be remarked that, from a macroscopic thermodynamic point of view, the model used is capable of giving a correct description of the phase diagrams and the thermodynamic properties of mixed crystals in the orientationally disordered state.

Further work has to be carried out to correlate the validity of the perhaps too simple assumed temperature function $g(T)$, as well as, in such a case, to verify the up to date experimental evidence of Eq. [8].

ACKNOWLEDGMENT

This work has been supported by the Spanish Dirección General de Investigación para la Ciencia y la Tecnología under Grant PB95-0032.

REFERENCES

1. J. Timmermans, *J. Phys. Chem. Solids* **18,** 1 (1961).
2. S. Urban, *Adv. Mol. Relax. Int. Proc.* **21,** 221 (1981).
3. J. N. Sherwood, "The Plastically Crystalline State." Wiley, New York, 1979.
4. N. G. Parsonage and L. A. K. Staveley, "Disorder in Crystals." Clarendon, Oxford, 1978.
5. A. Würflinger, *Int. Rev. Phys. Chem.* **12,** 89 (1993).
6. M. Barrio, D. O. López, J. Ll. Tamarit, P. Negrier, and Y. Haget, *J. Solid State Chem.* **124,** 29 (1996).
7. M. N. Akimov, O. F. Bezrukov, O. V. Chikunov, and A. V. Struts, *J. Chem. Phys.* **95**(1), 22 (1991).
8. A. R. Britcher and J. H. Strange, *J. Chem. Phys.* **75,** 2029 (1981).
9. H. M. Boots and P. K. de Bokx, *J. Phys. Chem.* **93,** 8240 (1989).
10. J. Ll. Tamarit, M. Barrio, D. O. López, and Y. Haget, *J. Appl. Crystallogr.* **30,** 118 (1997).
11. T. Calvet, M. A. Cuevas-Diarte, H. E. Gallis, and H. A. J. Oonk, *Recl. Trav. Chim. Pays-Bas* **115,** 333 (1996).
12. W. J. M. van der Kemp, J. G. Blok, P. R. van der Linde, H. A. J. Oonk, A. Schuijff, and M. L. Verdonk, *Calphad* **18,** 255 (1994).
13. D. O. López, J. van Braak, J. Ll. Tamarit, and H. A. J. Oonk, *Calphad* **19,** 37 (1995).

14. H. A. J. Oonk, T. Calvet, W. J. M. van der Kemp, and M. L. Verdonk, *in* "XIXèmes Journées d'étude des equilibres entre phases" (M. A. Cuevas-Diarte, J. Ll. Tamarit, and E. Estop, Eds.), p. 355. Barcelona, 1993.
15. M. Barrio, J. Font, D. O. López, J. Muntasell, J. Ll. Tamarit, N. B. Chanh, and Y. Haget, *J. Chim. Phys.* **87,** 1835 (1990).
16. H. A. Rose and A. van Camp, *Anal. Chem.* **28,** 1790 (1956).
17. M. Barrio, J. Font, D. O. López, J. Muntasell, J. Ll. Tamarit, P. Negrier, and Y. Haget, *J. Phys. Chem. Solids* **55,** 1295 (1994).
18. J. Salud, Doctoral thesis, Barcelona, in preparation.
19. D. Eilerman, R. Lippman, and R, Rudman, *Acta Crystallogr. Sect. B* **39,** 263 (1983).
20. N. Doshi, M. Furman, and R. Rudman, *Acta Crystallogr. Sect. B* **29,** 143 (1973).
21. R. Zannetti, *Acta Crystallogr.* **14,** 203 (1961).
22. V. H. P. Frank, K. Krzemicki, and H. Völlenke, *Chem. Z.* **97,** 206 (1973).
23. M. Barrio, D. O. López, J. Ll. Tamarit, P. Negrier, and Y. Haget, *J. Mater. Chem.* **5,** 431 (1995).
24. J. van Braak, D. O. López, and H. A. J. Oonk, unpublished results.
25. D. Chandra, W. Ding, and R. A. Lynch, *J. Less Common Metals* **168,** 159 (1991).
26. M. Barrio, J. Font, D. O. López, J. Muntasell, J. Ll. Tamarit, P. Negrier, N. B. Chanh, and Y. Haget, *J. Phys. Chem. Solids* **54,** 171 (1993).
27. S. Urban, J. Domoslawski, and Z. Tomkowiz, *Mater. Sci.*, **IV/3,** 91 (1978).
28. J. Bouwstra, N. Brouwer, A. C. G. van Genderen, and H. A. J. Oonk, *Thermochim. Acta* **38,** 97 (1980).
29. H. A. J. Oonk, "Phase Theory." Elsevier Science, Amsterdam, 1981.
30. L. Robles-Beneyt, Doctoral thesis, Bordeaux, 1995.
31. J. S. van Duijnevldt, F. S. A. Baas, and H. A. J. Oonk, "Prophase, an MS-DOS Program for the Calculation of Binary T–X Phase Diagrams." University of Utrecht, 1988.
32. W. J. M. van der Kemp, J. G. Blok, P. R. van der Linde, H. A. J. Oonk, A. Schuijff, and M. L. Verdonk, *Thermochim. Acta* **225,** 17 (1993).
33. D. O. López, J. van Braak, J. Ll. Tamarit, and H. A. J. Oonk, *Calphad* **18,** 387 (1994).
34. J. van Braak, D. O. López, J. Salud, J. Ll. Tamarit, M. H. G. Jacobs, and H. A. J. Oonk, *J. Crystallogr. Growth*, in press.